Sintering of Titanium with Yttrium Oxide Additions for the Scavenging of Chlorine Impurities

R.J. LOW, M. QIAN, and G.B. SCHAFFER

Chloride impurities in titanium powders are extremely difficult to remove and present a long-standing problem in titanium powder metallurgy. We show that the detrimental effects of chlorides on the sintering of titanium can be mitigated with trace additions of yttrium oxide, which has a high affinity for the normally volatile species and forms highly stable oxychloride reaction products. Compacts that would otherwise exhibit gross swelling and excessive porosity due to chloride impurities can be now sintered to near full density by liquid phase sintering. The potency of yttrium oxide additions is observable at levels as low as 500 ppm. The scavenging of chlorine by Y_2O_3 appears to be independent of alloy composition and sintering regime. It is effective when used with high-chloride powders such as Kroll sponge fines but ineffective when used with powders containing NaCl impurities or during solid-state sintering. The identification of highly potent chlorine scavengers may enable the future development of chloride-tolerant powder metallurgy (PM) alloys aimed at utilizing low-cost, high-chloride powder feedstocks.

I. INTRODUCTION

POWDER metallurgy (PM) is a promising avenue to low-cost titanium products. The appeal of PM methods is associated with potential cost and energy savings compared to traditional methods of manufacture based on repeated ingot metallurgy.[1–4] Such potential savings are derived principally from more efficient processing conditions, reduced material wastage, and the benefits of avoiding bulk melting of titanium.

Chlorine impurities have been a significant technical challenge in titanium production ever since the inception of the Kroll[5] and Hunter[6] processes themselves. Immediately after thermochemical reduction, the titanium product exists as a porous mass of metal (termed "sponge"), intermingled with chloride byproducts ($MgCl_2$ or NaCl) and excess reactants. The removal of the residual chlorides is one of the most difficult and expensive processes in the production of titanium sponge.[7] Purification, principally by vacuum distillation, is an energy-intensive batch process operated at elevated temperatures (107 K to 1233 K [800 °C to 960 °C]) over several days.[8]

Since complete removal of chloride impurities from titanium sponge is either not possible or not feasible, powders derived directly from sponge retain substantial levels of chloride. This includes sponge fines containing up to 1800 ppm of Cl[9,10] and hydride-dehydride (HDH) powder derived from the milling of sponge containing up to 600 ppm of Cl. Powders made from bar stock or ingots are regarded as essentially chloride free.[11–13] This includes PREP powder, gas atomized powder, and milled ingot metallurgy material (*via* the HDH process). However, these powders are significantly more expensive.

The high volatility associated with residual chlorides causes a variety of detrimental effects during subsequent processing.[4,14,15] Even at levels as low as 50 ppm, chloride impurities in PM products cause porosity,[16–18] microinclusions,[16,19,20] grain boundary embrittlement,[13,16,20] and poor weldability.[4,12,17] The effects of chlorides on sintering are most significant in the presence of liquid.[21–23] For example, chloride volatilization during liquid phase sintering leads to the formation of very large pores (sometimes millimeters in size) that are few in number.[21,23] Chlorine concentrations greater than 50 ppm are reported to cause severe sputtering and a highly porous weld zone during fusion welding. Mitigation techniques such as degassing of powders prior to sintering have very limited efficacy.[16,22,24] High-purity powders can be used to avoid these problems,[4,11,17,25] but since they are often derived from conventional ingot metallurgy, any potential savings associated with PM are lost.

With the goal of developing a cost-effective means of manufacturing titanium, we report in this study on the potential of yttrium oxide (Y_2O_3 or yttria) as a scavenger for chlorine during the sintering of titanium.

II. EXPERIMENTAL PROCEDURES

Three different titanium powders were used, and details are given in Table I. HDH titanium powder from

R.J. LOW, formerly Ph.D. Candidate, with The University of Queensland, School of Mechanical and Mining Engineering, ARC Centre of Excellence for Design in Light Metals, Brisbane, QLD 4072, Australia, is now Engineer with the Materials Technology Group, GHD Pty. Ltd., Brisbane, QLD 4000, Australia. M. QIAN, Reader in Materials Engineering and G.B. SCHAFFER, Professor, are with The University of Queensland, School of Mechanical and Mining Engineering, ARC Centre of Excellence for Design in Light Metals. Contact e-mail: ma.qian@uq.edu.au

Table I. Chemical Analysis of Titanium Powders; All Measurements are Given in ppm by Weight Unless Otherwise Specified

	Cerac Ti Powder (−100 Mesh)	Wuyi-Ti Sponge Fines (−2 mm)	Sodium-Reduced HDH Ti Powder (−100 Mesh)
O	2500	2000	2100
N	100	120	120
C	110	220	90
S	<10	<10	10
Cl	210	750	1300
Na	<5	12	1100
Mg	64	1500	<10

Cerac Inc. (Milwaukee, WI) was used predominantly. Kroll sponge fines from Wuyi-Ti (Kimet Special Metal Powder Co. Ltd., Wuyi, Hebei, China) and sodium-reduced HDH titanium powder from Lockheed Martin/ Oak Ridge National Laboratory (Oak Ridge, TN) were also used. Chemical analysis of the minor elements in the titanium powders was conducted by ATI Wah Chang (USA). Silicon (Cerac; −325 mesh, 99.5 pct pure) and nickel (Cerac; −325 mesh, 99.9 pct pure) powders, supplied by Cerac Inc., were used for alloying. Y_2O_3 powder (−10 μm) was supplied by Alfa Aesar (Ward Hill, MA). Powders were blended in a Turbula mixer for 30 minutes and compacted in a cylindrical floating die (10 mm diameter) at 400 MPa using a Carver hydraulic press. A suspension of Acrawax C in acetone was applied to the die and punch walls to lubricate the assembly during compaction. The compacts were ~10 mm in length and had a green density of ~74 pct theoretical.

Vacuum sintering was conducted in a Carbolite STF 15/450 alumina tube furnace under a vacuum of ~5 mPa. The furnace was held at 1473 K to 1673 K (1200 °C to 1400 °C) for 1 hour with a heating and cooling rate of 4 °C/min. To prevent bonding of the titanium to the furnace furniture, samples were placed on sintered yttria pieces.

The sintered density was determined by the Archimedes method as per Metal Powder Industries Federation Standard 42, with the exception that H-Galden ZT-180 high-density fluid (1.693 g/cm³ at 298 K [25 °C]) was used instead of water. The theoretical (or pore-free) density of alloys was calculated[26] using information from the phase diagram (i.e., the mass fraction of phases) and the density of the phases. The density of α-Ti, Ti_5Si_3, and Ti_2Ni was taken as 4.51 g/cm³,[27] 4.310 g/cm³,[28] and 5.723 g/cm³,[29] respectively.

Specimens for metallographic investigation were cut longitudinally along the axis of compaction and mounted in Bakelite. Polished samples were examined unetched. Macrographs were generated by stitching several overlapping optical images together. These are presented in the text with the same orientation as that during sintering. Porosity in the macrographs was quantified using ImageJ analysis software (National Institutes of Health, Bethesda, MD). Specimens for scanning electron microscopy (SEM) were coated with carbon and examined in a JEOL JSM-6460LA or a

JEOL 7001F SEM (JEOL Ltd., Tokyo, Japan), fitted with energy-dispersive spectroscopy (EDS) detectors. PRZ standardless quantitative analysis was used for oxygen-containing phases. Silicon in yttrium-containing phases was not quantified since the SiKα and YL1 X-rays have a similar energy. EDS spot analysis of particles in the matrix was conducted at 10 kV with a dwell time of 60 seconds. At this accelerating voltage, the electron beam interaction volume determined by Monte Carlo simulation for a flat Y_2O_3 substrate was approximately 1 μm. Particles smaller than this were omitted from the analysis.

Thermo-Calc TCW5 (TTTI3 database; Thermo-Calc Software, Stockholm, Sweden) and thermochemical HSC 7.0 software packages were used to estimate the liquid fraction and to calculate the Gibbs free energy of reaction, respectively.

III. RESULTS

A. Solid-State Sintering

To test the effect of rare earth oxides on solid-state sintering, elemental titanium was prepared with and without Y_2O_3 additions. Compacts without Y_2O_3 attained a relative density of 93.1 pct after sintering at 1673 K (1400 °C) for 2 hours. Given the particle size and compaction pressure used, the relative density achieved is consistent with other sintering studies.[9,13,30] The addition of 500 ppm Y_2O_3 did not alter the sintered density of unalloyed compacts. However, an appreciable level of chlorine was detected in the Y_2O_3 particles after sintering at both 1473 K (1200 °C) and 1623 K (1350 °C) (Figure 1).

B. Liquid Phase Sintering

The Ti-5Si alloy[21,23] forms ~32 wt pct liquid at 1623 K (1350 °C). These compacts bulge substantially during sintering and form excessively large pores that are millimeters in size (Figure 2(a)). However, trace additions of Y_2O_3 (500 ppm) lead to a dramatic change in the macrostructure. Figure 2(b) shows that samples with 500 ppm Y_2O_3 contain significantly smaller pores (~200 μm in diameter), and most of these pores are located towards the centre of the compact. The macrostructure shown in Figure 2(b) contains 1.2 area pct porosity by image analysis.

The effect of Y_2O_3 trace additions on densification is further demonstrated in Figure 3. The mean relative density of the Ti-5Si alloy is 77.1 pct; however, there is significant compact-to-compact variation. Relative densities for this alloy range between 74.1 and 78.8 pct. Trace additions (500 ppm) of Y_2O_3 resulted in near full density and a reduction in the compact-to-compact variation after sintering. The relative sintered density measured by the Archimedes method (shown in Figure 3) appears to be slightly different to that measured via image analysis. The small discrepancy (~0.7 percentage points) may be due to slight uncertainty in the theoretical density of the Ti-5Si alloy.

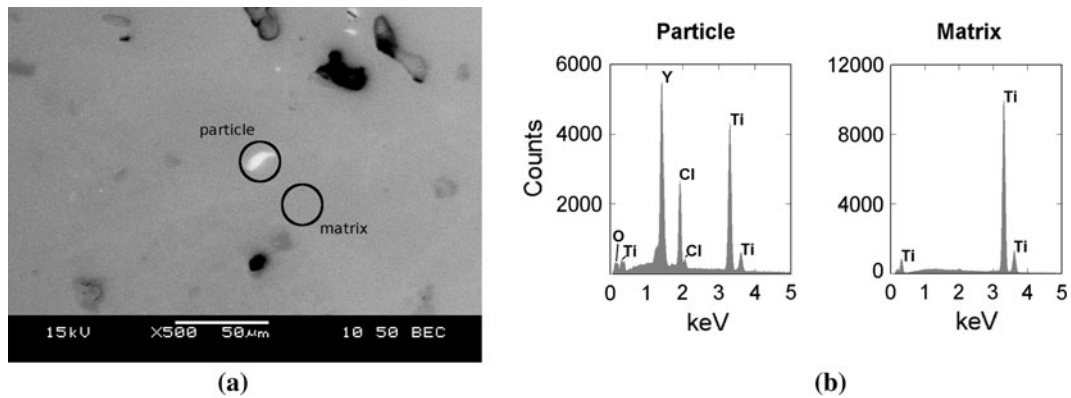Fig. 1—(a) SEM (unetched) micrograph of unalloyed titanium sintered with 500 ppm Y_2O_3 at 1673 K (1400 °C) for 2 h. EDS spectra of a second-phase particle and the adjacent matrix are shown in (b).
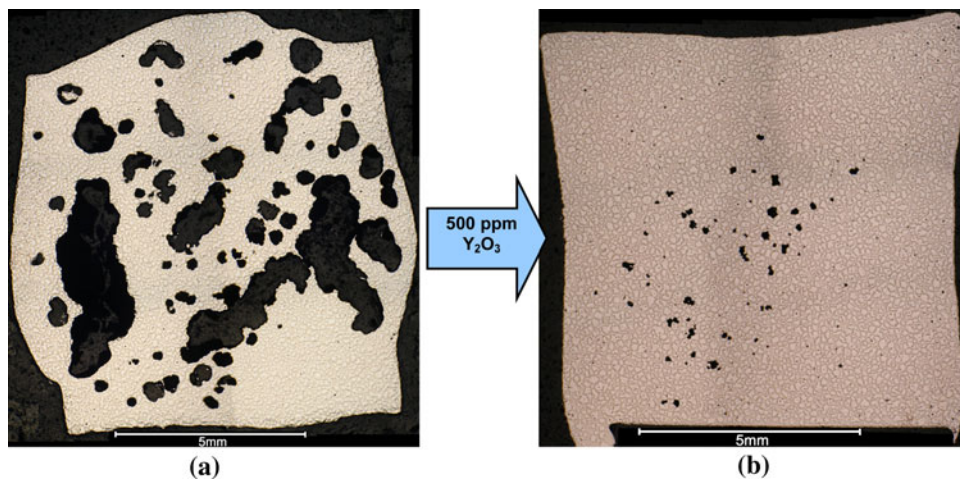

Fig. 2—Macrographs of Ti-5Si without and with 500 ppm Y_2O_3 additions are shown in (a)[23] and (b), respectively. Compacts were sintered at 1623 K (1350 °C) for 1 h. Porosity in the sample shown in (b) measured by image analysis is 1.2 pct by area.
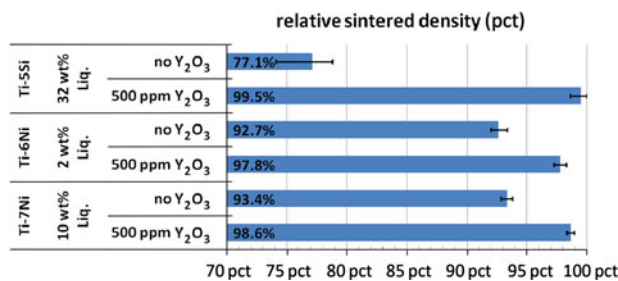

Fig. 3—Mean relative density of various Ti-Si and Ti-Ni alloys. The Ti-Si alloys were sintered at 1623 K (1350 °C) for 1 h, while the Ti-Ni alloys were sintered at 1573 K (1300 °C) for 1 h. Measurements were taken from at least three samples under each different condition. Error bars indicate the range of values.

Ti-Ni alloys[22] during liquid phase sintering also demonstrate a dramatic increase in sintered density with a trace addition of Y_2O_3. At 1573 K (1300 °C), the Ti-6Ni and Ti-7Ni alloy form approximately 2 wt pct and 10 wt pct liquid, respectively. Trace additions (500 ppm) of Y_2O_3 causes an increase in sintered density greater than 5 percentage points in both cases. The Ti-7Ni alloy,

for example, attains a sintered density of ~98.6 pct with 500 ppm Y_2O_3 powder.

The effect of Y_2O_3 additions during liquid phase sintering was also investigated in the Ti-4Si alloy[23] (Figure 4). When sintered at 1623 K (1350 °C), the alloy contains approximately 8 wt pct liquid. Samples without Y_2O_3 have a population of small rounded pores with an occasional large, elongated pore. Compacts with 500 ppm Y_2O_3 show noticeably less porosity and have none of the large elongated pores.

The improvement in sintered density was confirmed by density measurements. After sintering without Y_2O_3 additions, the Ti-4Si alloy attains an average density of 92.1 pct. The addition of 500 ppm Y_2O_3 increased the sintered density by approximately 3.6 percentage points. The compact-to-compact variation in density was also reduced. Attempts to increase sintered density by adding more Y_2O_3 were unsuccessful (Figure 5). On the contrary, there is possibly a slight decrease in sintered density with increasing amounts of Y_2O_3. Concentrations below 500 ppm were not experimentally feasible.

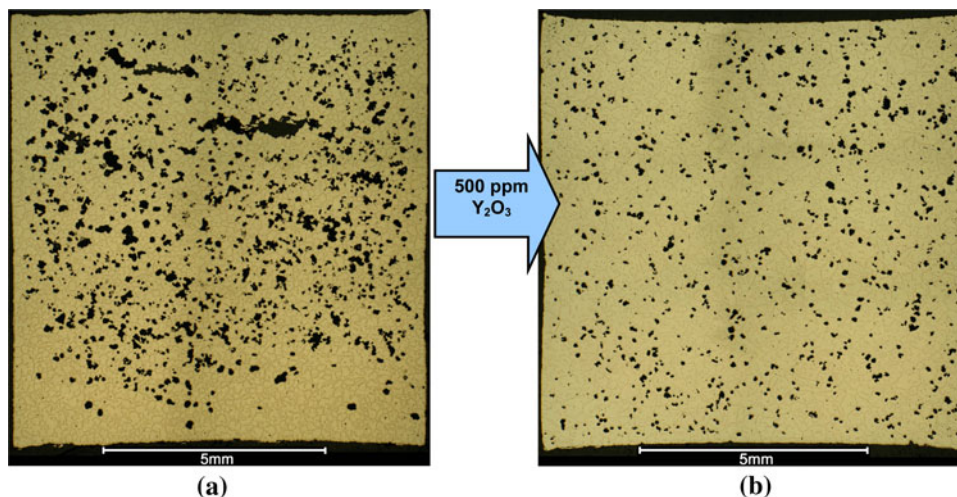A cluster of secondary phase particles in the Ti-4Si alloy with 500 ppm Y_2O_3 additions is shown in

Fig. 4—Macrographs of Ti-4Si without and with 500 ppm Y_2O_3 additions are shown in (*a*) and (*b*), respectively. Compacts were sintered at 1623 K (1350 °C) for 1 h.
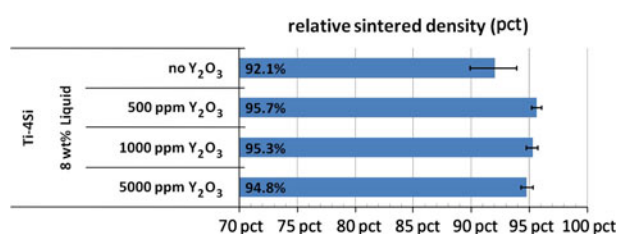

Fig. 5—Mean relative density of Ti-4Si sintered at 1623 K (1350 °C) for 1 h. Measurements were taken from at least three samples under each different condition. Error bars indicate the range of values.

Figure 6(a). These particles typically range in size from submicrometer to several micrometers. A range of morphologies was observed, including thin plates, rods, and spheres. The size and morphologies of the particles observed in the sintered microstructure were vastly different to the starting powder. The relatively large, round particle near the top right of Figure 6(a) is shown again in Figure 6(b) at a higher magnification. Standardless EDS spot analysis showed it to contain yttrium, oxygen (approximately 37 at. pct in both cases), and a substantial amount of chlorine, approximately 25 at. pct. Three types of particles were found in the microstructure. Most contain chlorine with a similar composition to that shown in Figure 6(b). The variation in composition among particles was less than 1.5 at. pct for each element. The second type of particle contains sulfur in addition to titanium (*e.g.*, Figure 7). The scavenging of sulfur by Y_2O_3 in titanium and other systems has been reported elsewhere[31–33] and is not the focus of this study. Finally, a small number of particles contains neither chlorine nor sulfur (here termed NCS particles) and have a composition that closely matches that of Y_2O_3.

At higher Y_2O_3 concentrations, a substantial portion of second-phase particles are found located within pores (Figure 8(a)). Most contain neither chlorine nor sulfur; however, some chlorine-containing particles are occasionally observed. The secondary phase particles observed within pores have a smooth, globular morphology (Figure 8(b)). This is different to the original Y_2O_3 powder particles, which have a fine, flake-like morphology.

C. Vacuum Degassing

Figure 9 compares the effectiveness of trace additions of Y_2O_3 with a prolonged intermediate temperature vacuum soak prior to sintering. Samples were soaked at 923 K (650 °C), 1273 K (1000 °C), and 1573 K (1300 °C) for 4 hours at each temperature. Compacts of both Ti-4Si and the Ti-5Si reached a similar sintered density to compacts treated with Y_2O_3 and sintered conventionally. Figure 10 shows the macrostructure of Ti-5Si following sintering after the prolonged intermediate temperature vacuum soak. The macrostructure of this alloy is similar to that of the same alloy sintered with 500 ppm Y_2O_3 (Figure 2(b)). The intermediate temperature hold has eliminated swelling and excessive porosity. Pores are few in number and centrally located. The pores are approximately 300 μm in size, slightly larger than that the same alloy sintered with 500 ppm Y_2O_3 (~200 μm).

D. Other Powders

To confirm whether the effects of Y_2O_3 observed so far are unique to the particular titanium powder used, two additional sources of powder were also tested. Sponge fines from Wuyi-Ti had a very coarse particle size relative to the silicon powder used for alloying. These powders were made by the Kroll process and contained approximately 750 ppm Cl. HDH powder derived from sodium-reduced sponge was also available. The powder had a similar particle size to the Cerac titanium powder (−100 mesh) and contained approximately 1300 ppm Cl.

These powders were blended with elemental silicon and sintered above the solidus. Sticking of compacts to the refractory and general buttressing indicated liquid
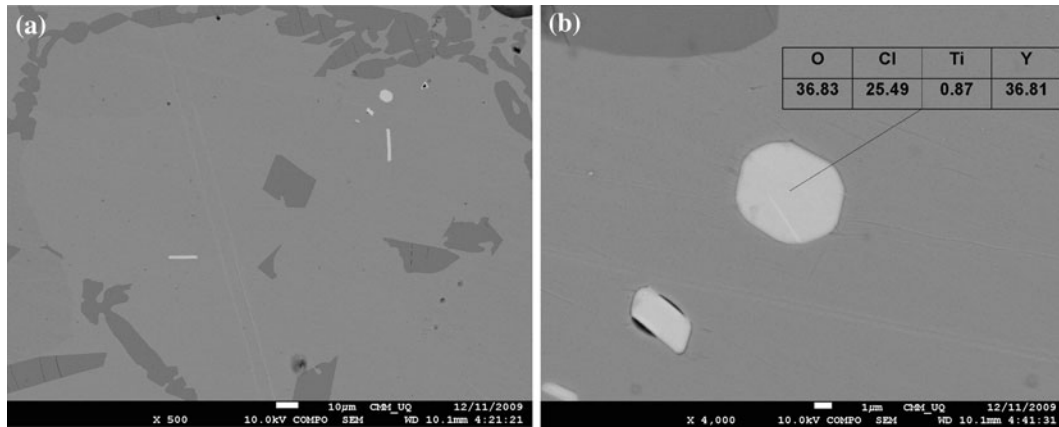
Fig. 6—SEM micrographs of Ti-4Si with 500 ppm Y_2O_3 sintered at 1623 K (1350 °C) for 1 h. A low magnification image is shown in (*a*). The large, round particle near the top right of (a) is shown at a higher magnification in (*b*). Standardless EDS analysis results are given in at. pct.
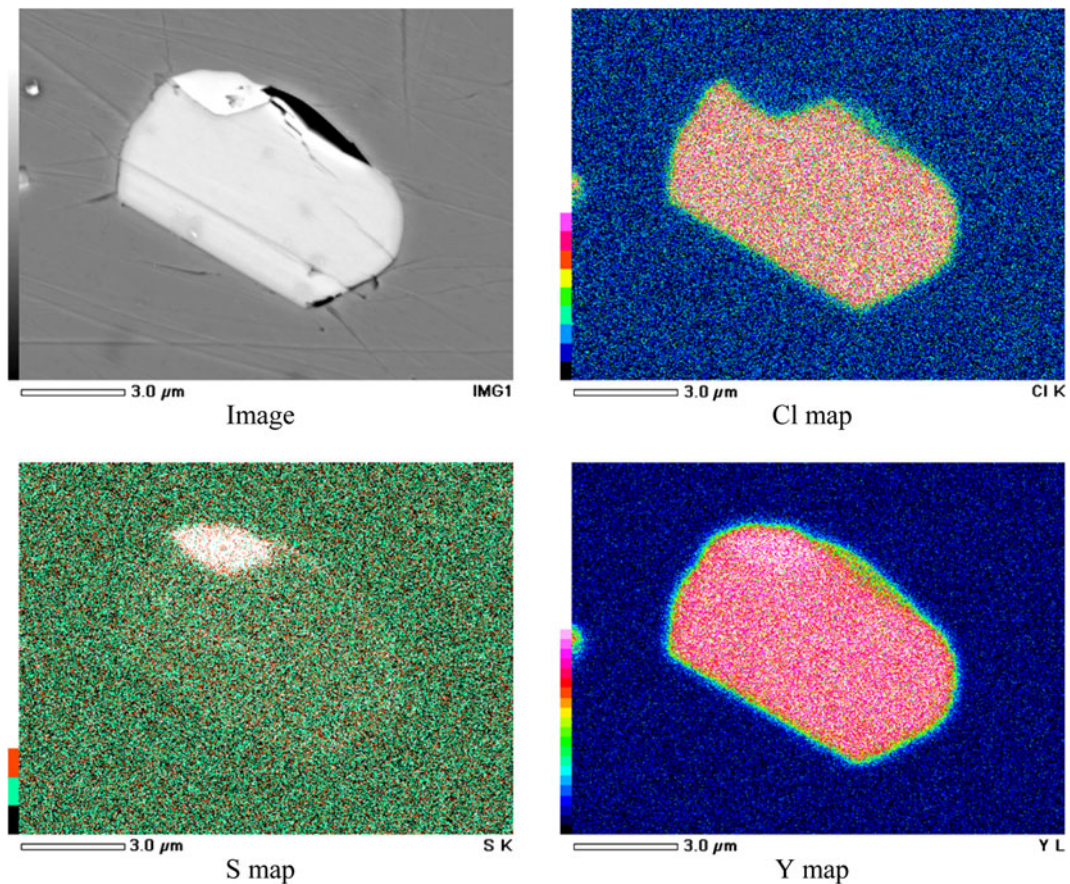

Fig. 7—EDS map of an yttria particle containing two phases, showing one part to be enriched in chlorine and the other in sulfur.

had formed in all cases during sintering. Figure 11 shows the effect of Y_2O_3 additions on the relative density of sintered compacts. Trace additions of Y_2O_3 to Ti-5Si compacts from Kroll sponge fines increased the relative sintered density by 6.1 percentage points. However, trace additions of Y_2O_3 had no effect on the sintered density of Ti-4Si compacts made with sodium-reduced HDH powder, even when a greater concentration of Y_2O_3 was used (5000 ppm or 0.5 wt pct).

IV. DISCUSSION

A. *Scavenging of Chlorine Species*

Residual magnesium chloride in titanium sponge from the Kroll process vaporizes during vacuum distillation at ~1173 K (~900 °C).[34,35] The formation of giant pores and swelling during titanium liquid phase sintering is thus thought to be due to the *in situ* volatilization of likely residual $MgCl_2$.[22] Thermodynamic data on the
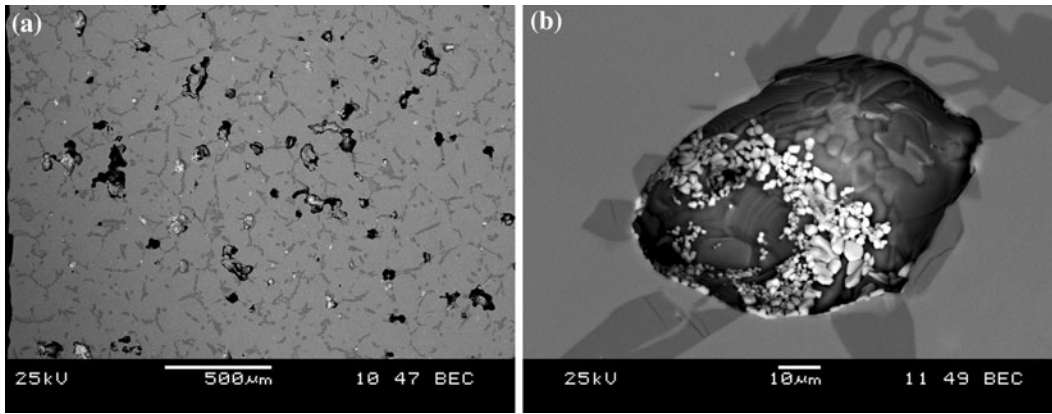
Fig. 8—SEM micrographs of Ti-4Si with 5000 ppm Y_2O_3 sintered at 1623 K (1350 °C) for 1 h showing secondary phase particles. A low-magnification image is shown in (a), and an image of the internal pore surface is shown in (b).
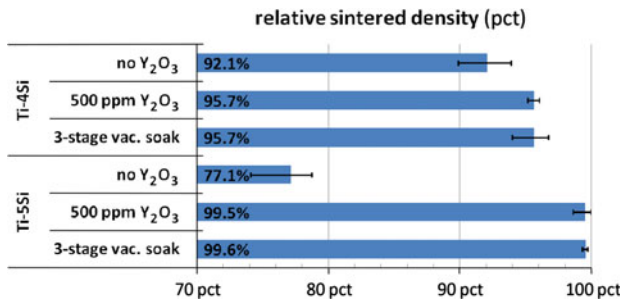

Fig. 9—Mean relative density of Ti-4Si and Ti-5Si sintered at 1623 K (1350 °C) for 1 h. Samples treated with a three-stage vacuum soak were heated to 923 K (650 °C), 1273 K (1000 °C), and 1573 K (1300 °C) each for 4 h, prior to sintering at 1623 K (1350 °C) for 1 h. Measurements were taken from at least three samples under each different condition. Error bars indicate the range of values.

formation of oxychloride (YOCl) appears to be very limited.[34,35] The thermochemical HSC 7.0 database gives the Gibbs free energy information about the reaction between Y_2O_3 and $MgCl_2$ at room temperature only.

$$Y_2O_3 + MgCl_2 = 2YOCl + MgO$$
$$\Delta G^\circ_{RXN}(25°C) = -49.4 \text{ kJ/mol}$$
[1]
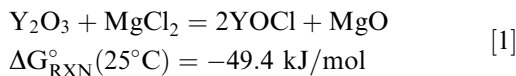
Increasing the reaction temperature typically accelerates the reaction. We therefore assume that Reaction [1], supported by the YOCl product observed in the as-sintered microstructure, has occurred during sintering at 1573 K (1300 °C). In addition, the Ellingham diagram of the Y_2O_3-Cl_2-O_2 system up to 1273 K (1000 °C) (Figure 12), produced by Gaviria and Bohe,[36] indicates that when Y_2O_3 is exposed to a chlorine gas-containing environment, the most stable product should be YOCl.

The enhanced densification observed is thought to be due to the scavenging of chlorine species by Y_2O_3 additions according to Reaction [1]. During sintering, the Y_2O_3 particles absorb the chlorine species and form stable, nonvolatile YOCl reaction products. This effectively dechlorinates the material, thereby reducing or eliminating entrapped gas. The most prominent example
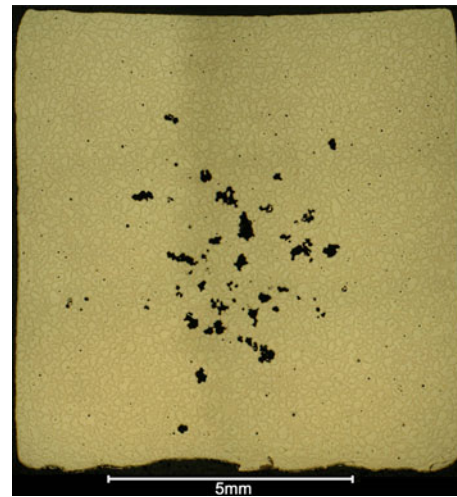

Fig. 10—Macrograph of Ti-5Si, heated to 923 K (650 °C), 1273 K (1000 °C), and 1573 K (1300 °C) each for 4 h, prior to sintering at 1623 K (1350 °C) for 1 h. Porosity in the sample measured by image analysis was 1.8 area pct.
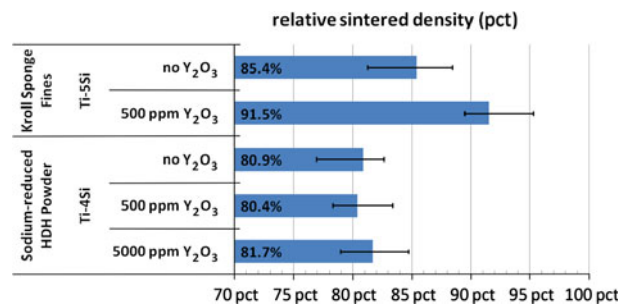

Fig. 11—Mean relative density of Ti-4Si and Ti-5Si sintered at 1623 K (1350 °C) for 1 h. Compacts consisted of powder from different sources. Measurements were taken from at least three samples under each different condition. Error bars indicate the range of values.

of the effect of chlorine scavenging is seen during the sintering of Ti-5Si at 1623 K (1350 °C) for 1 hour (Figure 2). Trace additions of Y_2O_3 to this alloy resulted
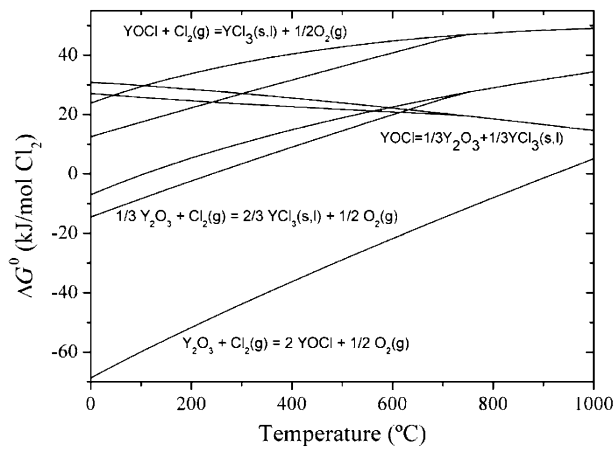
Fig. 12—Ellingham diagram of the (a) Y_2O_3-Cl_2-O_2 system, taken from Gaviria and Bohe.[36]

in near full density and the elimination of giant pores. A dramatic improvement in sintered density is also observed in Ti-Ni alloys and the Ti-4Si alloy. The chlorine scavenging also appears to reduce the significant compact-to-compact variation in density after sintering.

The presence of chlorine-containing particles in unalloyed titanium during solid-state sintering suggests the scavenging of chlorine species is not alloy specific or dependent on the type of sintering regime, even though the improvement in density is negligible after sintering in the solid state. During solid-state sintering, the strength of the interparticle bonds is expected to be significantly higher than that of the liquid bridges that develop during liquid phase sintering and will be large relative to the partial pressure of the chlorides. Thus, the entrapped gas has little effect during solid-state sintering at the relative densities studied in this article,[17] and its removal is therefore of little consequence.

This study has observed that YOCl particles are present in titanium after 60 minutes of sintering at temperatures up to 1673 K (1400 °C) despite the high affinity of titanium for oxygen. This indicates that YOCl is a stable phase in titanium up to 1673 K (1400 °C). However, it should be pointed out that the chlorine-scavenging process of Y_2O_3 may release some oxygen to the surrounding titanium matrix because the more stable YOCl phase contains less oxygen than Y_2O_3.

The observation of NCS particles perhaps indicates that some excess or unreacted Y_2O_3 particles are present in the microstructure. This is supported by the observation that the frequency of NCS particles increases when more Y_2O_3 powder is added with no improvement to sintered density. It is also observed that the composition of chlorine-containing particles appears to have a fixed maximum of approximately 25 at. pct. These observations seem to indicate the chlorine-scavenging process in titanium has reached completion at the lowest addition of Y_2O_3 powder.

Gaviria and Bohe[36] studied chlorination of Y_2O_3 up to a temperature of 1248 K (975 °C). In brief, they heated Y_2O_3 powder in a flowing gas mixture of argon

and chlorine at a rate of 3.8 °C/min—a similar heating rate as used in this study. Their thermogravimetric and X-ray diffraction experiments revealed that the transformation of Y_2O_3 into YOCl occurred quickly beyond 873 K (600 °C) and essentially completed at ~1103 K (~830 °C). This indicates that Y_2O_3 has high chemical affinity for Cl species even at temperatures much lower than the sintering temperature for Ti.

Y_2O_3 additions appear to have little effect as a chlorine scavenger on powders containing NaCl impurities in contrast to those containing $MgCl_2$. The thermochemical HSC 7.0 database similarly gives the Gibbs free energy information about the reaction between Y_2O_3 and NaCl at room temperature only.

$$Y_2O_3 + 2NaCl = 2YOCl + Na_2O$$
$$\Delta G^\circ_{RXN}(25°C) = 320.0 \, kJ/mol$$
[2]
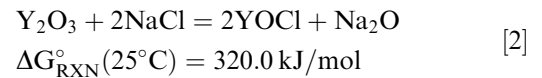
Compared to Reaction [1], the above reaction is much less favorable. This may help to understand the observation of Y_2O_3 being ineffective in scavenging chlorine in the form of NaCl.

B. Chloride-Tolerant Powder Metallurgy Alloys

The use of Y_2O_3 at trace levels offers a potentially fast and efficient means to mitigate volatile chloride impurities. Chlorine scavenging in Kroll powder also appears to be independent of alloy composition. Thus, a potential application for chlorine scavengers is the development of impurity-tolerant titanium alloys, particularly those sintered in the presence of a liquid. Sintering with a low liquid fraction is a conceivably viable method of rapidly attaining high densities while avoiding distortion and interactions with the support refractory. An alloy designed to form limited quantities of liquid may benefit from the use of Y_2O_3 additions.

Additionally, mill products made using PM techniques may also benefit from the use of chlorine scavengers. The poor weldability of titanium PM mill products has been a long-standing barrier to the development of the titanium PM industry.[4] Although the weldability of PM products was not the focus of this study, it has nevertheless been shown that trace additions of Y_2O_3 during elevated temperature processing are effective at binding chloride impurities in a stable, nonvolatile state. The use of chlorine scavengers presents a potentially novel solution to the significant problem of poor weldability in titanium mill products made directly from powder.

V. CONCLUSIONS

Trace additions of Y_2O_3 particles behave as highly potent chlorine scavengers during the sintering of titanium powder compacts. The Y_2O_3 reacts with chloride impurities forming stable, nonvolatile yttrium oxychloride compounds, which contain up to 25 at. pct chlorine. A substantial increase in sintered density during liquid phase sintering results from the gettering of the chlorine and the prevention of chloride vaporization.

Sintering to near full density (~99.5 pct) can be achieved with 500 ppm Y_2O_3 additions in compacts that would otherwise swell to ~77 pct relative density. The sintered density can be similarly improved by vacuum degassing for periods up to 12 hours at intermediate temperatures prior to sintering. The scavenging of chlorine with Y_2O_3 additions appears to be independent of alloy composition or sintering regime. The scavenging of chlorine with Y_2O_3 has a limited effect on densification during solid-state sintering because the pressure of the entrapped gas is negligible relative to the strength of the interparticle bonds. The Y_2O_3 treatment is also effective in the sintering of high-chloride-containing powders such as Kroll sponge fines, which contained approximately 750 ppm Cl. However, it is ineffective in powders containing sodium chloride rather than magnesium chloride. A chloride-tolerant PM alloy may enable the use of low-cost, high-chloride powder feedstocks.

ACKNOWLEDGMENTS

REFERENCES

1. M. Ashraf Imam and F. Froes: *JOM*, 2010, vol. 62, pp. 17–20.
2. M. Qian: *Int. J. Powder Metall.*, 2010, vol. 46 (5), pp. 29–44.
3. J.E. Barnes, W. Peter, and C.A. Blue: *Mater. Sci. Forums*, 2009, vols. 618–619, pp. 165–68.
4. National Materials Advisory Board, Appendix K: *Tonnage Powder Metallurgy DuPont Titanium Tonnage Powder Metallurgy. Titanium: Past, Present and Future*. National Academy Press, Washington, DC, 1983.
5. W. Kroll: U.S. Patent 2,205,854, 1940.
6. M.A. Hunter: *J. Am. Chem. Soc.*, 1910, vol. 32, p. 330.
7. V.A. Duz, O.M. Ivasishin, V.S. Moxson, D.G. Savvakin, and V.V. Telin: U.S. Patent 2009252638, 2009.
8. K. Shibata, H. Katayama, M. Yamaguchi, S. Takao, and S. Kosemura: *Titanium '95: Science and Technology*, presented at the Proc. 8th World Conference on Titanium, 1996, vol. 2, pp. 1543–50.
9. I.M. Robertson and G.B. Schaffer: *Powder Metall.*, 2010, vol. 53, pp. 146–62.
10. M. Qian, G.B. Schaffer, and C.J. Bettles: in *Sintering of Advanced Materials*, Z.K. Fang, ed., Woodhead Publishing Limited, Cambridge, 2010, pp. 323–54. ISBN: 1 84569 562 3.
11. F.H. Froes and D. Eylon: *Int. Mater. Rev.*, 1990, vol. 35, pp. 162–82.
12. A.D. Hanson, J.C. Runkle, R. Widmer, and J.C. Hebeissen: *Int. J. Powder Metall.*, 1990, vol. 26, pp. 157–64.
13. M. Kim, K. Vedula, P.C. Chen, and R. Bayer: *Prog. Powder Metall.*, 1986, vol. 41, pp. 173–86.
14. W.J. Kroll: *Metall*, 1957, vol. 11, pp. 1–7.
15. S.D. Hill and R.V. Mrazek: *Metall. Trans.*, 1974, vol. 5, pp. 53–58.
16. Z. Fan, H.J. Niu, B. Cantor, A.P. Miodownik, and T. Saito: *J. Microsc.*, 1997, vol. 185, pp. 157–67.
17. S. Abkowitz and D. Rowell: *J. Met.*, 1986, vol. 38, pp. 36–39.
18. I. Weiss, D. Eylon, M.W. Toaz, and F.H. Froes: *Metall. Trans. A*, 1986, vol. 17A, pp. 549–59.
19. K. Majima, T. Hirata, and K. Shouji: *J. Jpn. Inst. Met.*, 1987, vol. 51, pp. 1194–1200.
20. G. Welsch, W. Smarsly, and R. Borath: *Powder Metall. Int.*, 1982, vol. 14, pp. 190–94.
21. R.J. Low, I.M. Robertson, and G.B. Schaffer: *Scripta Mater.*, 2007, vol. 56, pp. 895–98.
22. I.M. Robertson and G.B. Schaffer: *Powder Metall.*, 2009, vol. 52, pp. 213–24.
23. R.J. Low, I.M. Robertson, M. Qian, and G.B. Schaffer: *4th Int. Conf. on Light Metals Technology*, 2009, vols. 618–619, pp. 509–12.
24. S.E. Rogers: *Powder Metall.*, 1961, vol. 4, pp. 249–67.
25. V.S. Moxson, P. Sjoblom, and M.J. Trzcinski: *Adv. Powder Metall. Part. Mater.*, 1992, vol. 6, pp. 125–40.
26. R.M. German: *Powder Metallurgy and Particulate Materials Processing*, Metal Powder Industries Federation, Princeton, NJ, 2005.
27. G. Lütjering and J.C. Williams: *Titanium*, Springer, New York, NY, 2003.
28. R.E. Kirk, D.F. Othmer, J.I. Kroschwitz, and M. Howe-Grant: *Kirk-Othmer Encyclopedia of Chemical Technology*, Wiley, New York, NY, 1991.
29. G.A. Yurko, J.W. Barton, and J.G. Parr: *Acta Crystallogr.*, 1959, vol. 12, pp. 909–11.
30. I.M. Robertson and G.B. Schaffer: *Metall. Mater. Trans. A*, 2009, vol. 40A, pp. 1968–79.
31. R.K. Dwivedi and D.A.R. Kay: *J. Less-Common Met*, 1984, vol. 102, pp. 1–7.
32. N. Liu, Z. Hu, K. Cui, X. Huang, and G. Zhang: *J. Rare Earths*, 1996, vol. 14, pp. 298–301.
33. B.W. Neuberger, P.G. Oberson, and S. Ankem: *Metall. Mater. Trans. A*, 2011, vol. 42A, pp. 1296–1309.
34. K. Shibata, M. Yamaguchi, H. Katayama, and N. Tokumitsu: *Mathematical Modeling for Vacuum Distillation in the Kroll Process*, Nippon Steel Technical Report, 2002, no. 85, pp. 36–40.
35. W.E. Wehn, G.B. Cobel, and W.E. Lusby: U.S. Patent 3,880,652, 1975.
36. J.P. Gaviria and A.E. Bohe: *Metall. Mater. Trans. B*, 2009, vol. 40B, pp. 45–53.